Journal of Theoretical and Applied Information Technology
30th September 2020. Vol.98. No 18

ISSN: 1992-8645 www.jatit.org E-ISSN: 1817-3195

DESIGN OF COMPOSITE MATERIALS USING INFORMATION TECHNOLOGY

[1]SERIK ZHUZBAYEV, [2]AKNUR ADILOVA, [3]SHYNAR AKHMETZHANOVA,

[4]BAKYT JUZBAYEVA, [5]DIANA SABITOVA.

[1,2,4]L.N.Gumilyov Eurasian National University, Nur-Sultan, Kazakhstan

[3]M.Kh.Dulati Taraz State University, Taraz, Kazakhstan

[5]Sh.Ualikhanov Kokshetau State University, Kokshetau, Kazakhstan

E-mail: [2]adilaknur_79@mail.ru

ABSTRACT

In this article, composite materials are considered, and the explicit difference scheme in solving dynamic problems of elasticity theory was developed on the basis of a combination of the spatial characteristics and the splitting methods, by extending the scope of its application to inhomogeneous linearly deformable bodies. This article discusses the stability of solving non-stationary problems of mechanics as applied to related problems of wave dynamics, and also compares the results of solutions obtained by the spatial characteristics method and the proven method, the algorithm for calculating the voltage at speeds at specific points, the situation at each special point with the interaction of a large number of nodes around her, communication and interaction.

The 21st century can be attributed to the age of composite materials. Today, without them, it is almost impossible to imagine the construction of industry, civil and residential complexes. Composites have entered and still enter our life and almost completely replace traditional materials in construction, energy, transport, electronics, etc.

Scientific and technical progress in the construction industry involves the usage of new and effective building materials with various complex of properties, different purposes.

Keywords: *Composite Materials, Mathematical Models, Study Area, Conditions, Medium, Difference Equation, Function.Tension, Speed, Numerical Solution*

1. INTRODUCTION

It's known that in a composition system such a composite materials in the vicinity of reinforcing elements implemented difficult tense-deformed condition, which determines working capacity of all introduction, in the end. However, there are only few jobs dedicated to detailed investigation of stress fields, strains around the fibers and investigation of mutual influences of these fields. Apparently, it's explained by extraordinary difficulty of stress distribution in the vicinity of fibers, especially near boundary surfaces and by learning difficulties.

As stated, it seems actual to hold such kind of investigations in the future.

XX'th century technical progress leaded to creation of new constructional materials with high specific strength and rigidity - composite materials or compositions.

Composite material is the material, which was made artificially, which consists of several components stayed separately at macroscopic level in the finish structure with well-observed border between them [2].

As a general rule, composite material (composition) consists of two categories of elements: reinforcing substance and matrix. Reinforcing substance provides a material with physical and mechanical properties, such a strength and elasticity. Matrix surrounds given substance with own material, providing a product with shape.

Compositional materials are divided into metallic and non-metallic matrixes (bases) with given distribution of reinforces (fiber, dispersed parts) in them. Herewith compositional materials allow to use individual properties of compositional components effectively. In a structural character compositional materials are subdivided into fibrous, hardened by continuous fibers and thready crystalls,

Journal of Theoretical and Applied Information Technology
30th September 2020. Vol.98. No 18

ISSN: 1992-8645 www.jatit.org E-ISSN: 1817-3195

dispersion hardened compositional materials, made by pressing or rolling of various materials.

Compositional materials are complicated materials, which include very different in components insoluble or sparingly soluble in each other components, that divided in strongly marked borders [2].

Compositional materials' properties depend on physicomechanical properties of components and connection strength between them. Distinctive feature of compositional materials is in value of components, not in their disadvantages. At the same time compositional materials possess properties, which aren't familiar to another components. Sharply differed components with additional features are selected to optimize properties.

To solve non-stationary problems in elastic media, one of the most convenient methods in applications is the bi-characteristics method using the ideas of the splitting method developed by G.T. Tarabrin [16]. An explicit difference scheme based on the bicharacteristic method with the use of the idea of splitting in spatial coordinates is adopted. Resolving difference equations are obtained for internal, boundary, angular, singular, and contact points of conjugation of a strip and a half-plane. To simulate the process of stress relief on a crack, singular generalized functions are used according to the method proposed in [5].

2. FORMULATION OF THE PROBLEM

Homogeneous isotropic band with rectangular cross section partially embedded in a homogeneous isotropic half-plane (take a look to Fig.1) [1], [5], [6]. Let coordinate (i=1,2) in a Cartesian systemoccupies the area $D_1 = \{0 \le x_1 \le L \cap |x_2| \le 1\}$ and the half-plane -

$D_2 = \{L_1 \le x_1 < \infty \cap |x_2| < \infty\}$.

Property of linear elastic isotropical heterogeneous (k=1,2) materials occupies density ρ_k, by Lame parameter λ_k, μ_k. At moment of time t≤0 the body stays at a rest-

$$v_\alpha^{(k)} = 0, \quad \sigma_{\alpha j}^{(k)} = 0, \quad \alpha, j = 1,2; \; k = 1,2 \qquad (1)$$

where are $v_\alpha^{(k)}$, $\sigma_{\alpha j}^{(k)}$ the components of the velocity vector and the stress tensor in the k-body. At the moment of time t_{11} (n=1,2,...,N) the upper boundary $x_1 = 0, |x_2| \le 1$ of the rectangular strip is dynamically disturbed by normal stresses changing according to the law[4], [16].

$$\sigma_{11}^{(1)} = f(t), \qquad \sigma_{12}^{(1)} = 0 \qquad (2)$$

At times $t_{11} + \tau$ (n =1,2, ..., N), the boundary $x_1 = 0, |x_2| \le 1$ is "pulled out" by tensile stresses. The applied voltage changes according to the law (Fig.2).

Another boundary parts of heterogeneous body stay away from tension

$$\sigma_{ij}^{(2)} = 0 \quad (j = 1,2) \quad \text{at} \quad x_1 = L_1, \quad 1 \le |x_2| < \infty \qquad (3)$$

$$\sigma_{j1}^{(1)} = 0 \quad (j = 1,2) \quad \text{at} \quad 0 \le x_1 \le L_1, \quad |x_2| = 1 \qquad (4)$$

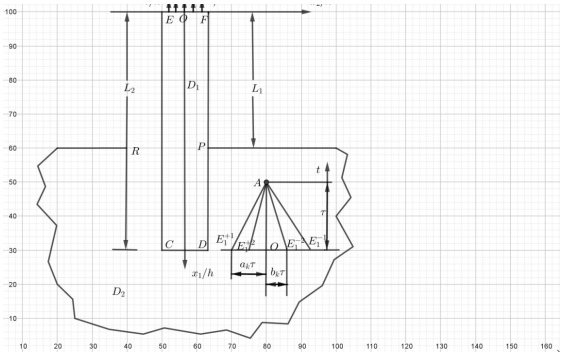

Figure 1. Study Area And Biocharacteristics

Conditions at contact borders meet the requirements of full adhesion of strip and half-plane.

$$v_\alpha^{(1)} = v_\alpha^{(2)}, \quad \sigma_{1j}^{(1)} = \sigma_{1j}^{(2)} \quad (\alpha, j = 1,2) \quad \text{at} \quad x_1 = L_2, \; |x_2| \le 1 \qquad (5)$$

$$v_\alpha^{(1)} = v_\alpha^{(2)}, \quad \sigma_{j2}^{(1)} = \sigma_{j2}^{(2)} \quad (\alpha, j = 1,2) \quad \text{at} \quad L_1 \le x_1 \le L_2, \quad |x_2| = 1 \qquad (6)$$

Here $f(t)$ is given boundary function and L_1, L_2, 1 are constant numbers, which determine sizes of strip and the contact area of heterogeneous environment.

Under the described conditions we need to research tense-deformed condition of $D_1 \cap D_2$ environment. To solve a given problem at the same time with initial problems (1) and boundary requirements (1) - (6) we use a system of equations, which include equations of movement and ratio of generalized law of Hook [3], [5], [19].

Journal of Theoretical and Applied Information Technology
30th September 2020. Vol.98. No 18

ISSN: 1992-8645 www.jatit.org E-ISSN: 1817-3195

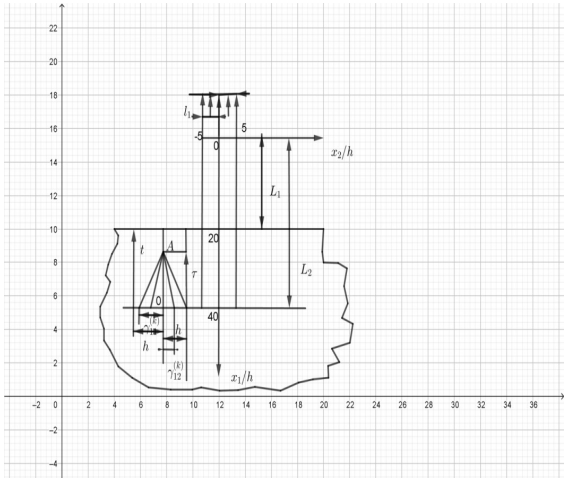

Figure 2. Study Area And Observation Points.

Here $f(t)$ is given boundary function and L_1, L_2, 1 are constant numbers, which determine sizes of strip and the contact area of heterogeneous environment.

Under the described conditions we need to research tense-deformed condition of $D_1 \cap D_2$ environment. To solve a given problem at the same time with initial problems (1) and boundary requirements (1) - (6) we use a system of equations, which include equations of movement and ratio of generalized law of Hook [7], [15], [17].

$$\rho_k v_\alpha^{(k)} = \sigma_{\alpha\beta,\beta}^{(k)}$$

$$\sigma_{\alpha j}^{(k)} = \lambda_k \varepsilon_{\beta\beta}^{(k)} \delta_{\alpha j} + 2\mu_k \varepsilon_{\alpha j}^{(k)} \qquad (7)$$

At $\varepsilon_{\alpha j}^{(k)} = 0.5\,(u_{\alpha,j}^{(k)} + u_{j,\alpha}^{(k)})$; δ_α - Kronecker symbol; $u_\alpha^{(k)}, \varepsilon_{\alpha j}^{(k)}$- components of displacement vector and deformation tensor. Indexes α, β, j take value 1,2; further takes value i is not equal to j: by lower indicates after the comma are indicated derivativesat relevant spacial coordinate; upper full stops mean derivatives of the time; its necessary to sum up by greek indexes that are repeated two times. In the end, index k determines possessment of point areas at strip (k=1) or half space area (k=2) is not equal.

The most comfortable way to find the solution of the problem is to have a look to dimensionless space of variables and desired parameters, which are obtained after entering the notation.

$$a_k = \frac{a_k^*}{a^*_m};\ b_k = \frac{b_k^*}{a^*_m};\ a_k^* = \left(\frac{\lambda_k + 2\mu_k}{\rho_k}\right)^{0.5}$$
$$b_k^* = \left(\frac{\mu_k}{\rho_k}\right)^{0.5};\ \rho_k = \frac{\rho_k^*}{\rho_{m^*}};\ a_m^* = \max(a_k^*);$$

$$x_i = \frac{x_i^*}{d^*};\quad v_\alpha^{(k)} = \frac{v_\alpha^{*(k)}}{a_{m^*}}$$
$$\sigma_{\alpha j}^{(k)} = \frac{\sigma_{\alpha j}^{*(k)}}{\rho_{m^*} a_{m^*}^{*2}};$$
$$\gamma_{11}^{(k)} = \gamma_{22}^{(k)} = \frac{\rho_k a^{*2} k^2}{a^{*2}_m};$$
$$\gamma_{12}^{(k)} = \gamma_{21}^{(k)} = \frac{\rho_k b^{*2} k^2}{a^{*2}_m};$$
$$\gamma_{33}^{(k)} = \gamma_{11}^{(k)} - 2\gamma_{12}^{(k)};\ t = \frac{t^* a_{m^*}}{d^*}; \qquad (8)$$

Here the index * is given to dimensions; the index m refers to the material in which the velocity of longitudinal waves stays the greatest; d* is a characteristic linear size; a_k, b_k are equal to the propagation speeds of longitudinal and transverse waves in the k-th medium; tia a time.

3. DETERMINING EQUATIONS OF THE DYNAMIC PROBLEM IN ELASTICITY THEORY

Using the relations (8) for dimensionless quantities, we are able to get from equations (7) after light transformations (i≠j):

$$\rho_k v_\alpha^{(k)} = \sigma_{\alpha\beta,\beta}^{(k)};$$

$$\sigma_{\alpha j}^{(k)} = (\gamma_{11}^{(k)} v_{j,j}^{(k)} + \gamma_{22}^{(k)} v_{j,i}^{(k)})\delta_{\alpha,j} + \\ + \gamma_{12}^{(k)}(v_{\alpha,j}^{(k)} + v_{j,\alpha}^{(k)})(1 - \delta_{\alpha j}) \qquad (9)$$

Equations (9) are a linear homogeneous hyperbolic system of first-order differential equations with constant coefficients [12], [18]

Its characteristic surfaces in three-dimensional space (x_1, x_2, t) they are hyper cones with axes parallel to the time axis (see Fig.3). The system of equations (9) has two branches in characteristic cones. These cones coincide with the bi-characteristics of equations (9). Along the bi-characteristics lying in the plane x_j=const, equations (9) are functions of only two variables (x_j;t). This process indicates that the conditions for a bi-characteristic can be obtained as conditions in the corresponding one-dimensional task. The corresponding transformations can be performed if one of the spatial variables is fixed in the system of equations (9). In this case, the system of equations (9) is split into two systems of equations corresponding to the directions j=1 and j=2 (i≠j):

$$v_\alpha^{(k)} - \rho_k^{-1} \sigma_{\alpha j,j}^{(k)} = A_{\alpha i}^{(k)}$$
$$\sigma_{\alpha j}^{(k)} - \gamma_{\alpha j}^{(k)} v_{\alpha j}^{(k)} = B_{\alpha j}^{(k)} \qquad (10)$$

Journal of Theoretical and Applied Information Technology
30th September 2020. Vol.98. No 18

ISSN: 1992-8645 www.jatit.org E-ISSN: 1817-3195

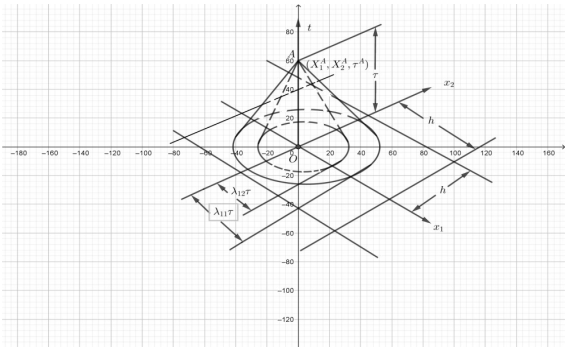

Figure 3. Characteristic Cones On The Plane

Where the notation is entered:

$$A_{\alpha i}^{(k)} = \rho_k^{-1}(\sigma_{\alpha\beta,\beta}^{(k)} - \sigma_{\alpha j,j}^{(k)})$$
$$B_{\alpha j}^{(k)} = \gamma_{22}^{(k)}\left(v_{\alpha,\alpha}^{(k)} - v_{\alpha,j}^{(k)}\right)\delta_{\alpha j} -$$
$$-\gamma_{12}^{(k)}\left(v_{i,j}^{(k)} - v_{j,i}^{(k)} - v_{\alpha,j}^{(k)}\right)(1-\delta_{\alpha j}) \quad (11)$$

Differential equations of characteristics have the form:

$$dx_\alpha = \pm\lambda_{\alpha j}^{(k)}\,dt \quad (12)$$

and the conditions for bi-characteristics are

$$d\sigma_{\alpha j,j}^{(k)} \pm (-1)\rho_k\lambda_{\alpha j}^{(k)}\,dv_\alpha^{(k)} =$$
$$= (B_{\alpha j}^{(k)} \pm ((-1)\rho_k\lambda_{\alpha j}^{(k)}A_{\alpha i}^{(k)})dt \quad (13)$$

Here $\lambda_{\alpha j}^{(k)} = \gamma_{11}^{(k)}$, if α = j, and $\gamma_{12}^{(k)}$, if α≠j. It can be seen from (12) that on each of the two hyperplanes there are two pairs of families of bi-characteristics defining longitudinal $\lambda_{jj}^{(k)}$ and shear $\lambda_{ij}^{(k)}\,(i \neq j, i,j = 1,2)$ velocities of wave propagation (see Fig.3). In each of the two planes (x_j; t) there are two families of behavioral characteristics of positive and negative directions. The sign at top corresponds to the behavioral characteristics of the positive, and the lower sign corresponds to the negative directions. Equations (12) and (13) correspond to each other for the same pair of indices and for the same arrangement of signs. We use equations (10) and conditions (13) to find a solution to the formulated problem (1) – (8).

4. SELECTING A POINT PATTERN FOR A TEMPLATE

In order to perform numerical calculations of the formulated problem for a region with a given configuration $D_1 \cap D_2$, it is necessary to study the characteristic surfaces [3], [5], [18]. The body $D_1 \cap D_2$ is subjected to non-stationary loads. The initial conditions (1) are given by the stresses and displacement velocities throughout the body, and the boundary conditions by the stresses on the surface (2) - (4). Both are seem to be continuous differentiable functions. The body structure is constructed toper mit existence of a coordinate system x_i(i=1,2), in which the boundary surfaces are coordinates. Let the body $D_1 \cap D_2$ be divided into cells formed by intersections of coordinate surfaces x_j=const(i=1,2). The linear dimensions of these cells in the direction of the axes x_1 and $x_2$are considered thought uniform and equal to h. The intersection of the lines x_j= const (i=1,2) form the nodes. At these nodal points , the values of the desired functions $v_\alpha^{(k)}, \sigma_{Aj}^{(k)}\,(\alpha, j = 1,2)$ are found at various points in time $t_n - \tau, t_n, t_n + \tau\ (n = 1,2,\ldots,N)$ with a time step of τ. The resulting grid is three-dimensional. The exact grid on the basis of which the difference scheme is constructed, in addition to the mentioned nodal points, contains points formed by the intersection of the bi-characteristics with hyperplanes t = const. Using an explicit difference scheme of the second order of accuracy makes it possible to establish the values of unknown quantities at the nodal points of the plane $t_n + \tau$ of the time layer from their known values at the nodes of the previous layer t_n. A template consisting of a node O and points $E_{\alpha j}^{\pm(k)}$, lying on the coordinate lines $x_j = const$ and separated from the point O by distances $\lambda_{11}^{(k)}\tau$ and $\lambda_{12}^{(k)}\tau$(Fig.4). Inclined straight lines starting from point A are bi-characteristics.

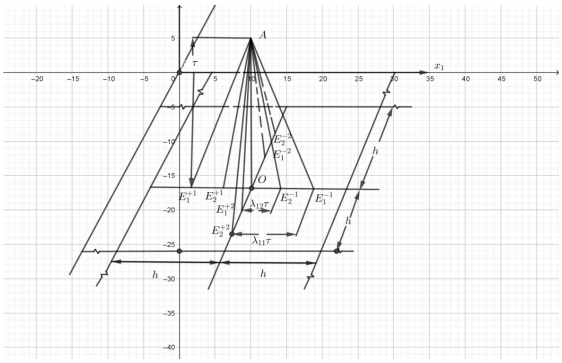

Figure 4. Point Grid Of The Difference Scheme For Internal Points.

In the future, the values of the functions at the point O are assigned the upper sign "O"; at the points $E_{\alpha j}^{\pm(k)}$- lower and upper sign ± (for example $\sigma_{\alpha j}^{\pm(k)}$),and no additional index is assigned at point A.

Journal of Theoretical and Applied Information Technology
30th September 2020. Vol.98. No 18

ISSN: 1992-8645 www.jatit.org E-ISSN: 1817-3195

A point grid of the difference scheme for internal node points is shown[8], [9], [10].

Points O and A represent the same point of the body at the same moments of time that are separated from each other by one step τ in time.

At the boundary points, the point network turns out to be somewhat different, since the boundary surfaces of the body cut off part of the bi-characteristics. So, for example, in Fig.5. a dot grid is shown for a nodal point lying on the boundary x_j=const, when the domain of definition is enclosed within $x_j \leq$const. In comparison with the internal nodes, there are no 4 bi-characteristics at the boundary nodal point that do not belong to the domain $D_1 \cap D_2$.

Looking at higher scatter of the schemes the method of solving dynamic problems allows to define the particle velocity $v_\alpha^{(k)}$ and the components of the stress tensor $\sigma_{\alpha j}^{(k)}$ at point A on the current layer at time t_n, if their values in the previous layer t_{n-1} $(n = 1, 2, \ldots, N)$ in point On and adjacent points, $E_{\alpha j}^{\pm(k)}$. Schemes that differentiate are called explicits. Explicit schemes are need able because there are no difficulties in solving the systems of difference equations associated with them. These systems are solved separatly from one time layer to the next. In this case, the desired values at each node, unlike the implicit difference scheme, are calculated independently of the others.

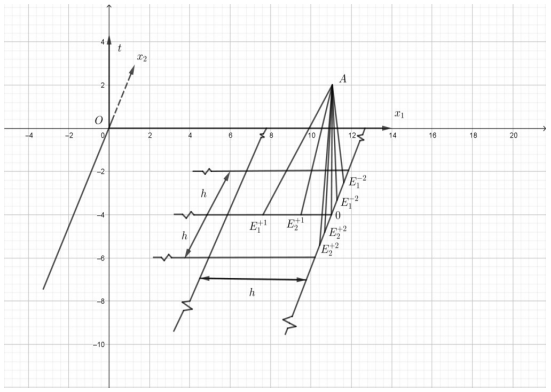

Figure 5. View Of The Bi-Characteristics On The Boundary Contour X_j = Const.

Schemes that distinguish are called explicits. Explicit schemes are necessary because there are no problems in solving systems of difference equations associated with them. These systems are solved separately from one time layer to another. In this case, the required values in each node, in contrast to the implicit difference scheme, are calculated independently of the others.

5. ALLOW A DIFFERENTIAL EQUATION TO SOLVE A DYNAMIC BOUNDARY VALUE TASKS

5.a. Resolving difference equations at internal points. The calculated algorithm of the second order of accuracy is constructed here [11], [14], [16]. Integrating a system of equations (10) from point O to point A and relations (13) from point $E_{\alpha j}^{\pm(k)}$ to point A by the trapezoid method (Fig.4) allows you to get expressions of the following type

$$v_\alpha^{(k)} = v_\alpha^{0(k)} + \frac{\tau}{2}\left(v_\alpha^{0(k)} + \rho_k^{-1}\sigma_{\alpha j,j}^{(k)} + A_{\alpha i}^{k}\right)$$
$$\sigma_{\alpha j}^{(k)} = \sigma_{\alpha j}^{0(k)} + \frac{\tau}{2}\left(\sigma_{\alpha j}^{0(k)} + \right.$$
$$\left. + \gamma_{\alpha j}^{(k)} v_{\alpha j}^{(k)} + B_{\alpha j}^{(k)}\right) \quad (14)$$

and

$$\sigma_{\alpha j,j}^{(k)} - \sigma_{\alpha j}^{\pm(k)} \pm (-1)\rho_k \lambda_{\alpha j}^{(k)} *$$
$$* \left(v_\alpha^{(k)} - v_\alpha^{\pm(k)}\right) = \frac{\tau}{2}\left(B_{\alpha j}^{(k)} + B_{\alpha j}^{\pm(k)} \pm\right.$$
$$\left. \pm(-1)\rho_k \lambda_{\alpha j}^{(k)}\left(A_{\alpha i}^{(k)} + A_{\alpha i}^{\pm(k)}\right)\right. \quad (15)$$

where the unknown values at point A are taken without additional indexes.

Values of functions at non-nodal points $E_{\alpha j}^{\pm(k)}$ are replaced with values calculated by the Taylor formula with accuracy to first order for the functions $A_{\alpha i}^{(k)}$ and $B_{\alpha j}^{(k)}$ and accurate to second order for functions $v_\alpha^{(k)}$ and $\sigma_{\alpha j}^{(k)}$ through their values at the nodal points O (x_1, x_2, t):

$$A_{\alpha i}^{\pm(k)} = A_{\alpha i}^{0(k)} \pm (-1)\lambda_{\alpha j}^{(k)} \tau \partial A_{\alpha j}^{(k)} / \partial x_j$$
$$B_{\alpha i}^{\pm(k)} = B_{\alpha i}^{0(k)} \pm (-1)\lambda_{\alpha j}^{(k)} \tau \partial B_{\alpha i}^{(k)} / \partial x_j \quad (16)$$

and

$$\sigma_{\alpha j}^{\pm(k)} = \sigma_{\alpha j}^{0(k)} \pm (-1)\lambda_{\alpha j}^{(k)} \tau \partial \sigma_{\alpha j}^{0(k)} / \partial x_j +$$
$$+0{,}5(\lambda_{\alpha j}^{(k)}\tau)^2 \partial^2 \sigma_{\alpha j}^{0(k)} / \partial x_j^{\,2},$$

$$v_\alpha^{\pm(k)} = v_\alpha^{0(k)} \pm (-1)\lambda_{\alpha j}^{(k)} \tau \partial v_\alpha^{0(k)} / \partial x_j +$$
$$+0{,}5(\lambda_{\alpha j}^{(k)}\tau)^2 \partial^2 v_\alpha^{0(k)} / \partial x_j^{\,2} \quad (17)$$

The partial derivatives of the system of equations (10) with respect to the variable x_j are written as

$$\partial v_\alpha^{0(k)} / \partial x_j = \rho_k^{-1} \partial \sigma_{\alpha j,j}^{0(k)} / \partial x_j + \partial A_{\alpha j}^{0(k)} / \partial x_j$$
$$\partial \sigma_{\alpha j}^{0(k)} / \partial x_j = \gamma_{\alpha j}^{(k)} \partial v_{\alpha j}^{(k)} / \partial x_j +$$

ISSN: 1992-8645 www.jatit.org E-ISSN: 1817-3195

$$+\partial B_{\alpha j}^{(k)}/\partial x_j \qquad (18)$$

Substituting relations (16), (17) in (15), and then eliminating with the help of (14) the variables $v_\alpha^{(k)}$; $\sigma_{Aj}^{(k)}$ and taking into account (18), we can obtain eight equations for the derivatives of $v_{\alpha j}^{(k)}$; $\sigma_{Aj,j}^{(k)}$, $A_{Ar}^{(k)}$, $B_{Aj}^{(k)}$ in the estimated layer time

$$\gamma_{\alpha j}^{(k)2} v_{\alpha j}^{(k)} \pm (-1)\lambda_{\alpha j}^{(k)} \sigma_{\alpha j,j}^{(k)} = \\ = \gamma_{\alpha j}^{(k)2}\left(v_{\alpha j}^{0(k)} + \tau\partial v_\alpha^{0(k)}/\partial x_j\right) \pm \\ \pm(-1)\lambda_{\alpha j}^{(k)}\left(\sigma_{\alpha j,j}^{0(k)} + \tau\,\sigma_{\alpha j}^{0(k)}/\partial x_j\right) \qquad (19)$$

By adding corresponding pairs of equations (19),we can find unknown derivatives

$$v_{\alpha j}^{(k)} = v_{\alpha j}^{0(k)} + \tau\partial v_\alpha^{0(k)}/\partial x_j \\ \sigma_{\alpha j,j}^{(k)} = \sigma_{\alpha j,j}^{0(k)} + \tau\partial \sigma_{\alpha j}^{0(k)}/\partial x_j \qquad (20)$$

The system of equations (20) can be used to define unknown derivatives both in the inner and boundary nodal points of area $D_1 \cap D_2$. Such expressions can be obtained directly by integrating the system of equations (9) according to the Euler scheme, first differentiating them by x_j. Whatever it is good to have intermediate relations (19), which are used in solving systems of equations where boundary functions are already there. Substituting the equalities (20) in (14) allows us to obtain unknown functions $v_\alpha^{(k)}$, $\sigma_{Aj}^{(k)}$ in the internal nodal points of a non-homogeneous body at the time $t_{n-1} + \tau\ (n = 1,2,\ldots,N)$.

5.b. Different equations at boundary points. On the boundary lines x_j= const , two voltage components are specified (see Fig.(2) – (4)) [4], [16]. The calculations aren't able to use conditions (19) on two bi-characteristics that do not belong to the domain $D_1 \cap D_2$ (Fig.5). Thus, in comparison with the internal points, the number of equations (19) is reduced to two. The complex of equations (19), (14), and two boundary conditions (2) – (4) (or (3)) are closed linear system with respect to unknowns (eight derivatives and five functions). The points of contact lines CR, PD and CD are also considered as boundary points only for certain regions $D_1 \cap D_2$. At each of these points, the number of equations (19), (14) is 22, and the unknown ones are 26. A closed system of equations is revealed if we use, not only equations (14), (19), but also four conditions for the rigid cordon of the band and the half-plane (5) or (6).

5.c. Different equations in non-singular angular points. At the angular points F and E, 4 components of the stress tensor are defined. According to the law of pairs of tangent stresses, only three of them become independent. The calculations as for conditions on 4 bi-characteristics that do not belong to the $D_1 \cap D_2$. The number of unknown derivatives can be reduced by direct differentiation of the boundary functions $(\sigma_{\alpha j}^{(k)}, \alpha \neq j)$ in (2), (4), the derivatives $\sigma_{12,1}^{(k)} = 0$ and $\sigma_{12,2}^{(k)} = 0$ are obtained. The unknowns revealed by solving equations (19) and (14) sequentially.

5.d. Different equations in special angular points. At the contact points (P,R,C,D) the inhomogeneous medium $D_1 \cap D_2$ has special features. In this term, we discuss features in contact points similar to points C and D of the problem that is studied. Contact points P and R have their own characteristics. Developing the ideas first described in, we calculate the difference equations at special angular points of the body under study [1], [7], [18]. At special points P and R , it is assumed from physical considerations that the stress components $\sigma_{12}^{(k)} = 0$ and $\sigma_{11}^{2} = 0$ are equal to zero and conditions (6), (4) are used. It is assumed that the region D_1 along the PR line is mentally divided into subregions (I), (II). Thus, near the singular points P and R, three subregions (I), (II), (III) are considered (see Fig.1). For subregions (I) and (II) we accept conditions for the continuity of functions.

$$v_\alpha^{(I)} = v_\alpha^{(II)};\ \sigma_{\alpha j}^{(I)} = \sigma_{\alpha j}^{(II)} \\ (\alpha, j = 1,2) \qquad (21)$$

and their derivatives

$$v_{\alpha,2}^{(I)} = v_{\alpha,2}^{(II)};\ \sigma_{\alpha 2,2}^{(I)} = \sigma_{\alpha 2,2}^{(II)} \\ (\alpha, j = 1,2) \qquad (22)$$

The derivatives $v_{\alpha,1}^{(I)}$ and $\sigma_{\alpha\,1,1}^{(I)}$ can be discontinuous. 12 unknown derivatives for medium I and 8 derivatives for medium II are calculated by the formula (20). Substituting into equation (14) the derivatives found in this way for each subdomain and fulfilling conditions (16), (21) and (22), unknown functions are calculated at points P and R, as in multiply connected nodes of the set of subdomains (I), (II), (III). For example

$$\sigma_{22}^{(1)} = \sigma_{22}^{(2)} = \left(\sigma_{22}^{0(1)} + \sigma_{22}^{0(2)}\right)/2 + \\ + \tau/2\left(\gamma_{33}^{(1)}\left(v_{1,1}^{(I)} + v_{1,1}^{(II)}\right)/4 + \gamma_{33}^{(2)} v_{1,1}^{(III)}/2 +\right.$$

ISSN: 1992-8645 www.jatit.org E-ISSN: 1817-3195

$$+(\gamma_{11}{}^{(1)}v_{2,2}{}^{(1)}+\gamma_{11}{}^{(2)}v_{2,2}{}^{21})/2+$$
$$+(\sigma_{22}{}^{0(1)}+\sigma_{22}{}^{0(II)})/4+\sigma_{22}{}^{0(III)}/2$$

The function $\sigma_{11}{}^{(k)}(k=1,2)$ suffer discontinuities at these points and have the form

$$\sigma_{11}{}^{(1)}=\sigma_{11}{}^{0(k)}+{}^{\tau}/_{2}\,(\gamma_{11}{}^{(1)}(v_{1,1}{}^{(I)}+$$
$$+V_{1,1}{}^{(II)})/2+\gamma_{22}{}^{(1)}V_{2,2}{}^{(1)}+\sigma_{11}{}^{0(I)}+\sigma_{11}{}^{0(II)},$$

where the upper Arabic numerals indicate that the corresponding parameters belong to the k-th medium (k=1,2), and Roman numerals for the i-th medium (I), (II), (III) the subregions.

At special corner points C and D the condition is assumed

$$v_{\alpha}{}^{(1)}=v_{\alpha}{}^{(2)};\quad \sigma_{\alpha j}{}^{(1)}=\sigma_{\alpha j}{}^{(2)} \qquad (23)$$

as a consequence of equalities (5) and (6) with respect to the 1st and 2nd medium.

Mentally dividing the neighborhood of points C and D in the second medium into three subregions (II, III, IV) extensions of the lines CR, PD, and CD for each subdomain of the 2nd medium use assumptions similar to those accepted at points P and R (conditions (21) and (22)) (see Fig.1).

During getting unknown functions $v_{\alpha}{}^{(III)}$; $\sigma_{\alpha j}{}^{(III)}\ (\alpha,j=1,2)$ in the points with a and D in subregion (III) derivatives of 1st and of 2nd order in equation (20) can not be calculated since these equations are linearly – independent for the respective common lines of subregions II and IV, and the second mixed derivatives are calculated separately, because central parts can not be used at all.

In subdomains II and IV, it is assumed that all 16 derivatives of $v_{\alpha j}{}^{(k)},\sigma_{\Delta j,j}{}^{(k)}\ (\alpha,j=1,2)$ suffer discontinuities.

For each of the subregions (I, II, III, IV) unknown functions and their derivatives are calculated by solving equations (20) and (14) sequentially, taking into account the above conditions for the subdomain (III). Conditions (21), (22) and (23), unknown functions at special points C and D are formed from a multi-connected system of equations for subdomains (I, II, III, IV). For example,

$$\sigma_{11}{}^{(1)}=\sigma_{11}{}^{(2)}=(\sigma_{11}{}^{0(1)}+\sigma_{11}{}^{0(2)})/2+$$
$$+\tau/4(\gamma_{11}{}^{(1)}v_{1,1}{}^{(I)}+\gamma_{22}{}^{(1)}v_{2,2}{}^{(1)}+\sigma_{11}{}^{0(1)}+$$
$$+\gamma_{11}{}^{(2)}(v_{1,1}{}^{(II)}++v_{1,1}{}^{(III)}+v_{1,1}{}^{(IV)})/3+$$
$$+\gamma_{22}{}^{(2)}(v_{2,2}{}^{(II)}+v_{2,2}{}^{(III)}+v_{2,2}{}^{(IV)})/3+$$
$$+(\sigma_{11}{}^{0(I)}+\sigma_{11}{}^{0(III)}+\sigma_{11}{}^{0(IV)})/3$$

About what was said in sections (a –d) it can be noticed that the unknown values of derivatives $v_{\alpha,j}{}^{0(k)},\sigma_{\alpha j,j}{}^{0(k)}$ at the nodal points of the study area $D_1\cap D_2$ are thought equal to the derivatives on the lower layer in time t_{n-1} (n=1, 2, ... N), which are solved using the central difference at the inner nodal points, and at the boundary points by corresponding approximations "forward" and "back".

6. ESTIMATION OF DYNAMIC STRIP "PULLING", PARTIALLY FIXED IN A HALF PLANE

Let's imagine a width made of a linearly elastic material, whose features are spoken by the density ρ_1, the velocity of propagation of longitudinal a_1 and the transverse b_1 waves in the stationary rectangle of coordinates x_1Ox_2 is the region $|x_2|\le 1,\ 0\le x_1\le\infty$ in the initial moment of time the body is at rest [16], [17], [18]:

$$v_{\alpha}=0,\sigma_{\alpha j}=0\ (\alpha,j=1,2)\ \text{for}\ t_0=0 \qquad (24)$$

At any other time $t_n+\tau$ (n=1,2,..., N) at the end $x_1=0$ of the half strip, the boundary condition (2) applies. The rest of the boundaries of a homogeneous body are stress free

$$\sigma_{22}=0,\sigma_{12}=0\ \text{for}\ |x_2|\le 1,0\le x_1\le\infty \qquad (25)$$

The problem is reduced to integrating the system of equations (7) under both initial (24) and boundary conditions (2) and (25).

The mathematical problem is formulated properly. At the initial moment of time $t_0 = 0$, the ground occupying the half-plane is at rest so that

$$v_0=0,\sigma_{\alpha j}=0\quad(\alpha,j=1,2) \qquad (26)$$

The impact tool action is modeled by the normal load perceived by the well base ($x_1=H,|x_2|\le 1$) and described like:

$$\sigma_{11}=1{,}7\ \text{if}\ 0\le t\le 450\tau,$$
$$\text{and}\ \ 0.\quad \text{if}\ t>450\tau;$$
$$\sigma_{12}=0 \qquad (27)$$

The surface of the well and surface of the ground are not loaded. Under the characterized conditions, it is necessary to investigate the stress-strain state of the soil, as well as establish the area and degree of compaction.

Journal of Theoretical and Applied Information Technology
30th September 2020. Vol.98. No 18

ISSN: 1992-8645 www.jatit.org E-ISSN: 1817-3195

The boundary value problem is formulated in the initial (1),boundary (3) - (4) and pin (5) – (6) conditions (see Fig.1). At time $t_n+\tau$ (n = 1,2, ..., N) the boundary $x_1=0$, $|x_2| \le 1$ (the end face of the inclusion EF) is "pulled out" by tensile stresses. The applied voltage varies according to the law (Fig.2).

$$\sigma_{11} = t\exp(-t), \text{ if } 0 \le t \le \tau_0, \text{ and } \tau_0\exp(-\tau_0), \text{ if } t > \tau_0$$
$$\tau_{12} = 0 \quad (28)$$

The parameter τ_0 determines the time moment after which the exponential nature of loading changes to a constant one (see the waveform of point 1 in Fig.7).

In order to save computer RAM, it was necessary to limit the computational domain to a boundary ($0 \le x_1 \le M_1, |x_2| \le M_2$), which is chosen so that the disturbances reflected from it at any time cannot distort the stress and velocity field in the entire region research $D_1 \cap D_2$. The calculations were studied for various configurations of inclusions [12], [16]. In Fig.6-8 and Fig.11-18 the calculation results are given for the following inclusion sizes 1=5h; L_1=20h and L_2=40h. In Fig.9 and 10 show the calculation results for the following inclusion sizes 1=3h; L_1=20h and L_2=25h.

Calculated waveforms of normal $\sigma_{ii}^{(k)}$ $(i=1,2)$ and tangents $\sigma_{12}^{(k)}$ voltage (k=1,2) at the time interval $0 \le t \le 140\tau$ in six fixed observation points: 1(x_1=0h, x_2=0h), 2(x_1=0h, x_2=3h), 3(x_1=10h, x_2=3h), 4(x_1=20h, x_2=3h), 5(x_1=30h, x_2=0h) and 6(x_1=45h, x_2=10h) are represented by curves in Fig.6-8. Oscillograms of normal $\sigma_{22}^{(1)}$ at fixed observation points are shown by the curves in Fig.6. The flat stress front by the boundary action at the end x_1 =0 comes sequentially to the layers at the x_1 coordinate.

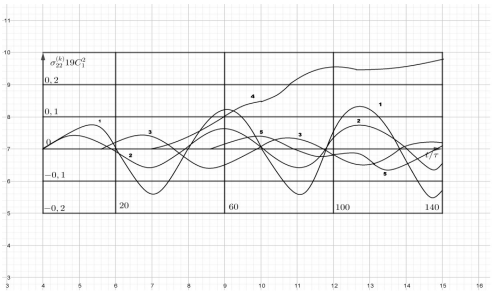

Figure 6. Oscillogram Of Normal Stresses $\sigma_{22}^{(k)}$ $(k=1,2)$

The action of wave fronts and their interaction with diffracted waves leads to the fact that the character of the change in normal stresses $\sigma_{22}^{(k)}$ they become alternating at the observed points 1, 2, 3, and 5. The sixth point is not shown in Fig.6. due to the smallness of their values, which is explained by a significant weakening of elastic perturbations as they pass into the region occupied by the matrix. At points 1, 2 and 3, starting from a certain point in time, symmetrical sinusoidal oscillations with respect to time are established at approximately constant amplitudes and frequencies at each point.

In addition, at points 1 and 2, vibrations are carried out the same frequencies. At point 5 (the contact surface), oscillations asymmetric that are not symmetrical in time are observed. Normal stress $\sigma_{22}^{(1)}$ at point 4, it remains tensile over time interval under consideration up to t=140τ. At the same time, the high voltage level $\sigma_{22}^{(1)}$ at point 4, it changes drastically from the stresses at other observation points and is explained by the influence of angular diffraction emanating from the singular point P.

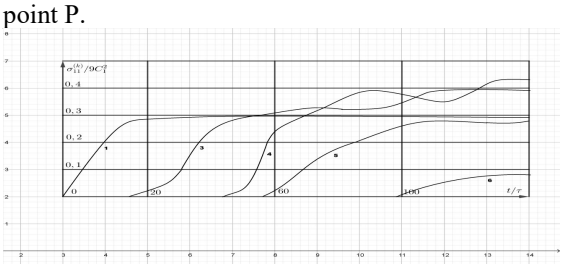

Figure 7. Waveforms Of Normal Stresses $\sigma_{12}^{(k)}(k=1,2)$ *At Fixed Six Points*

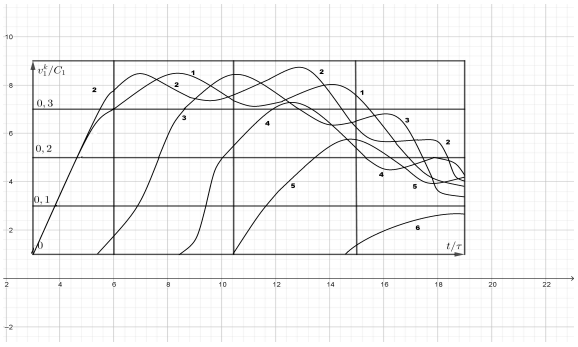

Figure 8. Waveforms Of Longitudinal Velocities $v_1^{(k)}$*(K=1, 2) At 6 Points: 1 .(X1=0, X2=0), 2.(X1=0, X2=3h), 3.(X1=10h, X2=3h), 4.(X1=20h, X2=3h), 5.(X1=30h, X2=0), 6.(X1=45h, X2=10h)*

ISSN: 1992-8645 www.jatit.org E-ISSN: 1817-3195

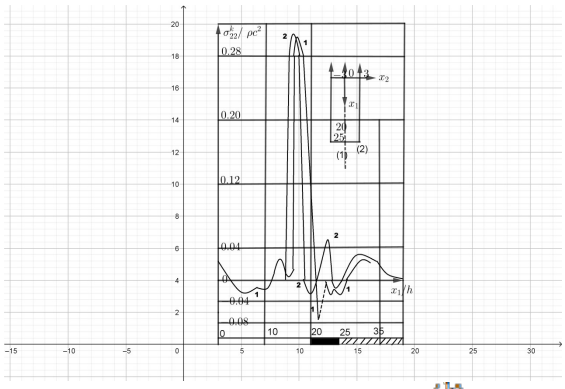

Figure 9. Changes in normal stresses $\sigma_{22}^{(k)}$ at time t=100 t in coordinate x_1 in sections 1(x_2=0h), 1'(x_2=0h), 2 (x_2=3h)

The normal stresses $\sigma_{11}^{(k)}$(k=1,2) at all points of the considered time interval is stretchable in accordance with the law of the acting load t exp(-t) (point 1). The values of normal stresses $\sigma_{11}^{(1)}$ at the boundary point 2 coincide with their values at the point 1 and therefore are not given [13], [18]. For small values of time, the behavior of the curves at points 3, 4, and 5 is determined by the plane tensile wave that comes from the end face x_1 = 0 the initial exponential nature of the pulse applied at the x_1 = 0 boundary comes sequentially to the underlying layers along the x_1 coordinate. At point 3 in the time interval up to t≤110τ due to the influence of diffracted waves, the normal voltage $\sigma_{11}^{(1)}$ it fluctuates around the average value, starting from the time t≥110τ, it is set at the same level. As for points 4 and 5, the described behavior of normal voltage $\sigma_{11}^{(1)}$ is repeated, but only at late points in time (t≥140τ). The behavior of the curve at point 4 differs from the stress changes at other points in that the vibrations are carried out with increasing amplitude. This circumstance is explained by the appearance of angular diffraction coming from the point P. At point 6, the level of normal stresses $\sigma_{11}^{(2)}$ is significantly lower than the stresses at points 1, 2, 3, 4 and 5. This is explained by a noticeable weakening of the elastic waves passing through the contact boundary of dissimilar materials and by the low rigidity of the matrix material. The delay effect of the appearance of the normal stress $\sigma_{11}^{(2)}$ is comparable with the behavior of other state parameters with the exception of the normal stress $\sigma_{22}^{(2)}$ (see Fig.6).The character of the change in the normal voltage of the normal voltage $\sigma_{11}^{(2)}$ repeats the form of the boundary action (point 1).

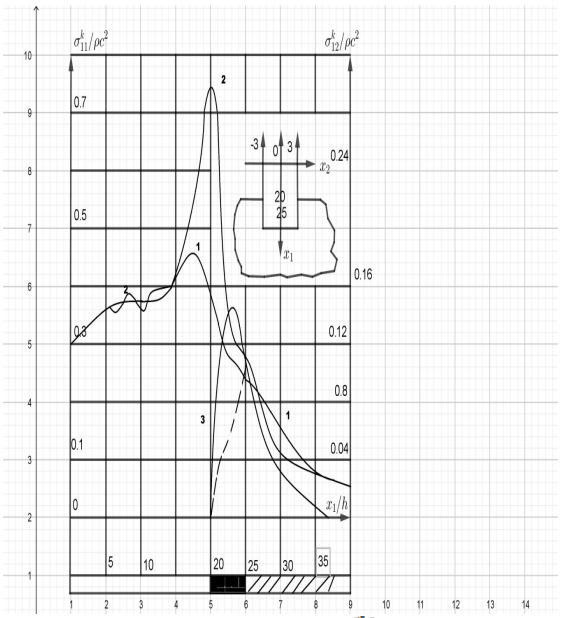

Figure 10. Changes in normal $\sigma_{11}^{(k)}$ (curves 1, 2) and tangents $\sigma_{12}^{(k)}$ stress at time t=100τ in coordinate x_1 in cross-sections 1(x_2=0h), 3'(x_2=3h), 2(x_2=3h)

Time evolution of longitudinal velocities $v_1^{(k)}$(k=1,2) particles at the accepted fixed observation points are shown by curves in Fig.8. At the initial stages of the movement, the longitudinal velocities $v_1^{(k)}$(k=1,2) at all observed points change smoothly, repeating the form of the applied boundary action. Increasing the time, they also become ready to global changes. The curves at the observed points, except for point 6, are intertwined with each other, passing later into oscillatory motion. This is explained by the superimposition of a longitudinal elastic wave front reflected from the junction boundary of dissimilar materials and diffracted waves differing from the angular points P and D. Thus, the determining influence on the formation of the longitudinal velocity at points 4, 5 and 6 is provided by the processes of reflection and refraction of elastic waves from the contact surfaces of heterogeneous materials.

Journal of Theoretical and Applied Information Technology
30th September 2020. Vol.98. No 18

ISSN: 1992-8645 www.jatit.org E-ISSN: 1817-3195

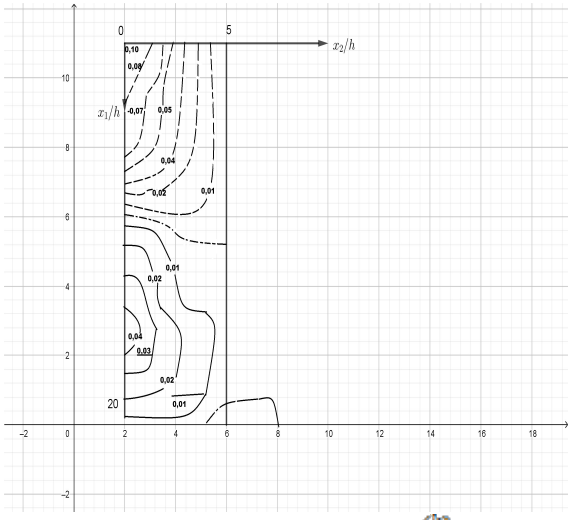

Figure 11. Isolines of normal stresses $\sigma_{22}^{(k)}$ (k=1,2) at time t= 40τ

In Fig.9 and 10 shows the change of the normal $\sigma_{ii}^{(k)}$(i=1,2) and tangents $\sigma_{12}^{(k)}$of the stresses (k=1,2) in coordinate x_1 in sections 1(x_2=0; section belonging to the inclusion); 1'(x_2=0; section belonging to the matrix material); 2(x_2=3h; cross section belonging to both the inclusionand the matrix material) at the time moment t=100τ. The normal component of the stress $\sigma_{22}^{(k)}$ (k=1,2; see Fig. 9) in section 1 in the area of the protruding part of the inclusion $0 \le x_1 \le L_1$ with an increase in x_1 goes from stretching to compressing with a small amplitude. Near the contact area $L_1 \le x_1 \le L_2$ the voltage level increases sharply. At the output of their contact region ($x_1 \ge L_2$), the normal component of the stresses $\sigma_{22}^{(k)}$ it is greatly reduced. In section 1', which belongs to the matrix material. The values of normal $\sigma_{22}^{(2)}$ differ from their values $\sigma_{22}^{(1)}$ during inclusion, when switching from inclusion in the matrix, the normal component of stresses $\sigma_{22}^{(k)}$changes with a abruptly. In section 2(x_2=3h) at the boundary of the inclusion and the matrix, the normal voltage $\sigma_{22}^{(k)}$accepts a null value on a free surface at $0 \le x_1 \le L_1$. In the contact area ($L_1 \le x_1 \le L_2$) it starts increasing sharply. At the same time, the stress levels in sections 1 and 2 differ not so much. At the exit from the contact zone ($x_1 \ge L_2$), the normal component of the stresses $\sigma_{22}^{(2)}$decreases strongly and has a negative value. In the area of the matrix, they change little and are oscillatory in nature. Fig.10 combined graphs of normal $\sigma_{11}^{(k)}$ and tangent $\sigma_{12}^{(k)}$ stresses (k =1,2) along the x_1 coordinate in the above sections are shown. The normal stresses $\sigma_{11}^{(k)}$(k=1,2) in sections 1 and 2 are stretchable. Near a singular point P (section 2), normal stresses $\sigma_{11}^{(k)}$take an extreme value that exceeds the nominal value by two times at the time under consideration.

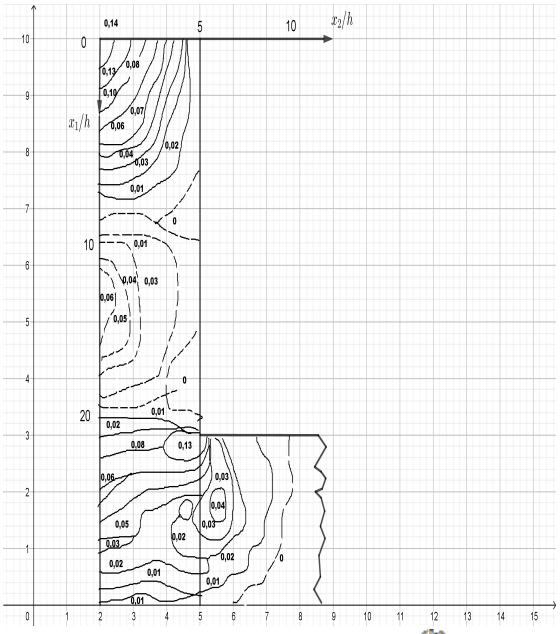

Figure 12. Isolines of normal stresses $\sigma_{22}^{(k)}$ (k=1,2) at time t= 60τ

Tangential stresses $\sigma_{12}^{(k)}$(k=1,2) in the contact area increase sharply from zero to its huge value and then slowly decrease to zero when entering the matrix material [1], [17]. The distribution of tangent stresses along the contact boundary of the inclusion and matrix in dynamic problems does not differ qualitatively from what occurs in the case of statics. The results illustrated by the calculated curves are consistent with the nature of the passing wave fronts.

Journal of Theoretical and Applied Information Technology
30th September 2020. Vol.98. No 18

ISSN: 1992-8645 www.jatit.org E-ISSN: 1817-3195

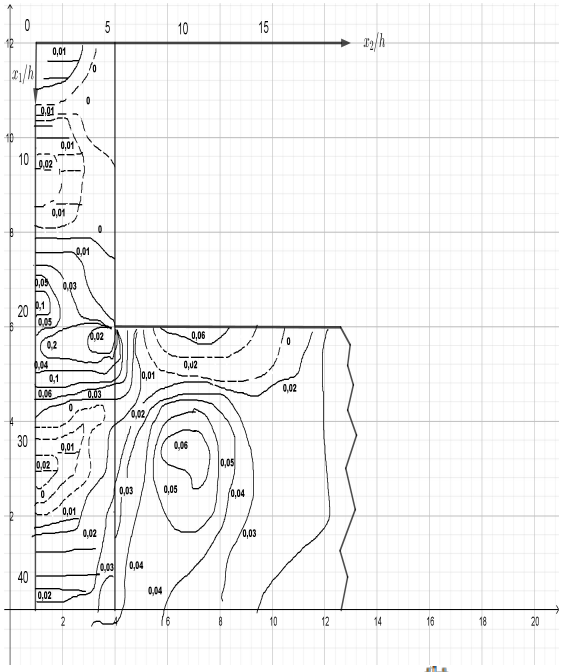

Figure 13. Isolines Of Normal Stresses $\sigma_{22}^{(k)}$ (K=1,2) At Time T= 100τ

In Fig.11-18 in the plane x_1Ox_2, the isolines of normal $\sigma_{ii}^{(k)}$ (i=1,2) and tangents $\sigma_{12}^{(k)}$ (k=1,2) determining the stress state in the entire region of the inhomogeneous medium $D_1 \cap D_2$ for individual moments of time. Constructed isolines of the stress tensor $\sigma_{\Omega j}^{(k)}$ allow you to reveal the most dangerous areas of the body $D_1 \cap D_2$ in terms of possible subsequent destruction. In contrast to the previously used in the presented figures, the following notation is used: solid, dashed, dashed and dashed lines indicate isolines corresponding to tensile, zero, and compressive stresses.

The evolution of the normal $\sigma_{22}^{(k)}$ and tangents $\sigma_{12}^{(k)}$ the stresses (k=1,2) at time points t=40τ, t=60τ and t=100τ are shown in Fig.11 – 16. From these figures, we can conclude that the constructed isolines correspond to the character of passing wave fronts caused by multiple reflections and diffraction of elastic waves from plane boundaries. In Fig.17– 18 the isolines of normal stresses $\sigma_{11}^{(k)}$ (k=1,2) at moments of time t=60τ and t=100τ. From the results shown in the figures, we can imagine a clear figure of the stress distribution in the vicinity of singular points, at the contact boundaries of dissimilar bodies. The regions of existence of significant stress gradients and their concentrations in the vicinity of corner points and at the contact boundaries of the inclusion and matrix are found. The normal stresses $\sigma_{11}^{(k)}$(k=1,2) in the entire region of the inhomogeneous body, they are stretchable at a time t=60τ and reach their maximum value equal to 0.48 at a particular point P. The effects of stress concentration in the vicinity of the singular point P are well illustrated by the contours shown in Fig.18.

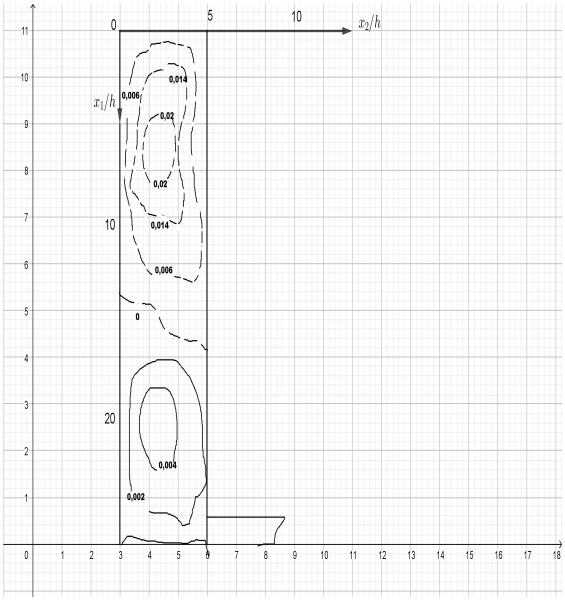

Figure 14. The Isolines For The Shear Stresses $\sigma_{12}^{(k)}$ (K=1,2) At Time T= 40τ

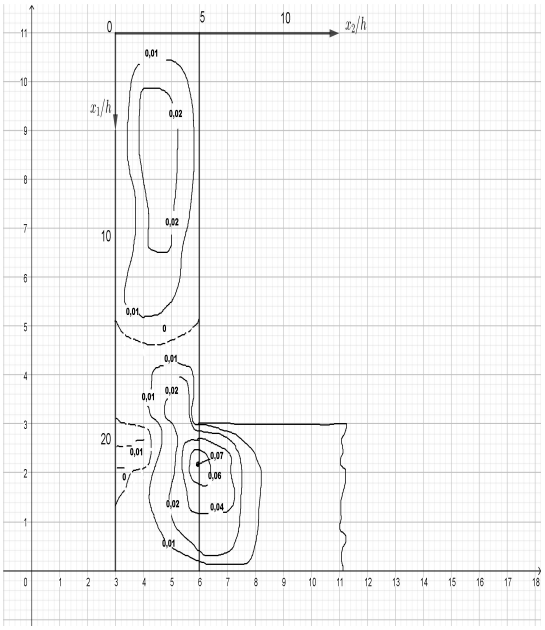

Figure 15. The Isolines For The Shear Stresses $\sigma_{12}^{(k)}$ (K=1,2) At Time T= 60τ

The stress level is a function of time and at different points in time reaches different values at different points of the inhomogeneous medium [15], [17].

ISSN: 1992-8645 www.jatit.org E-ISSN: 1817-3195

The normal stresses $\sigma_{11}^{(k)}$(k=1,2) reach their local extremum equal to 0.63 in the transition area from free areas to the contact area of the inclusion and matrix. At the same moment of time, near the inclusion end face, the contours take the form of straight lines, indicating the transition to a steady state, which is consistent with the external load specified at the boundary.

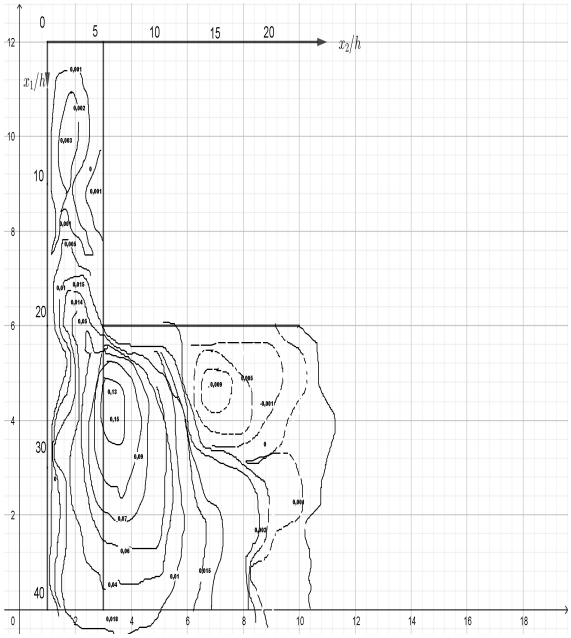

Figure 16. The Isolines For The Shear Stresses $\sigma_{12}^{(k)}$ (K=1,2) At Time T= 100τ

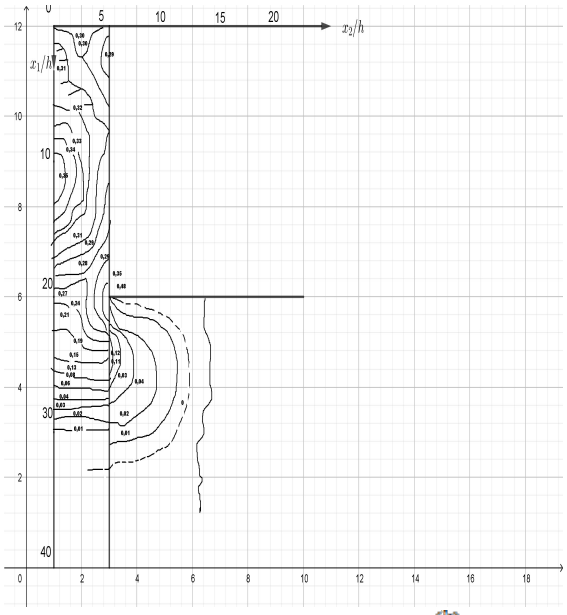

Figure 17. Isolines Of Normal Stresses $\sigma_{11}^{(k)}$ (K=1, 2) At Time T= 60τ

This analysis are part of phenomena of dynamic load transfer on composite materials' component elements and at the same time demonstrates the possibility and effectiveness of the developed mathematical models of non-stationary problems of elasticity theory.

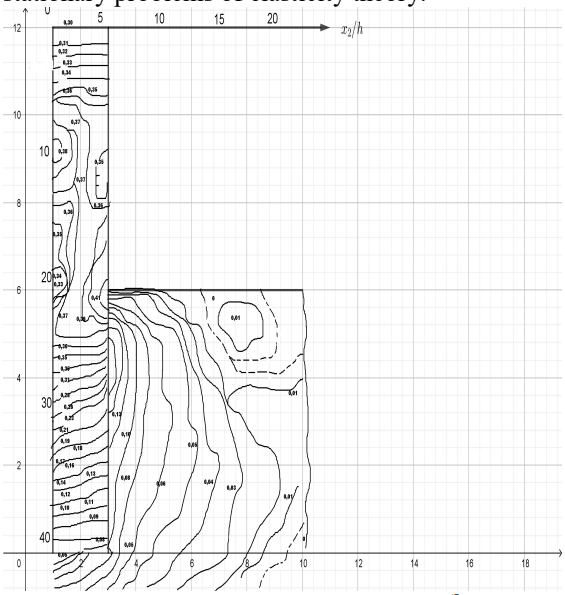

Figure 18. Isolines Of Normal Stresses $\sigma_{11}^{(k)}$ (10^{-2}; K=1,2) At Time T= 100τ

7. CONCLUSION

The basic results and analysis made under this theory, it allows us to reveal these conclusions:

An explicit difference scheme in solving dynamic problems in elasticity theory was developed on the basis of a combination of the spatial characteristics method and the splitting method, by extending the scope of its application to inhomogeneous linearly deformable bodies.

Applied to the contact problems of wave dynamics, the stability of the difference numerical solution of non stationary problems in mechanics is improved, which is shown in comparison of results of the solution obtained by the spatial characteristics method.

An algorithm for calculating stresses with velocities at special points, which are the corner points of a strip, a quarter of a plane, a half-plane with cuts and inserts, points of breaking of boundary conditions and the contact boundary of heterogeneous bodies, is developed nowadays. On the basis of the developed method, solving equations are obtained at the described special points and on contact surfaces. The state at each particular point is determined by the

ISSN: 1992-8645 www.jatit.org E-ISSN: 1817-3195

interconnectedness and mutual influence of a large number of nodal points located in its vicinity.

Based on the developed technique, resolving equations are obtained at the described singular points and on the contact surfaces. The state at each particular point is determined by the interconnectedness and mutual influence of a large number of nodal points located in its vicinity.

Based on the developed methods, a package of application programs in algorithmic language for solving dynamic problems in homogeneous and inhomogeneous bodies in a wide range of non-stationary external influences is revealed.

The phenomenon of dynamic stress concentration in the vicinity of singular points is established and their values are estimated under the conditions of solved partial problems.

REFERENCES:

[1] Bulatov V.V, Vladimirov Yu.V. Theory of wave motions of inhomogeneous media: monograph [Electronic resource]. – Kirov: MTSNIP, 2017.

[2] Bondaletova L.I., Bondaletov V.G. Polymer Composite Materials (part 1): tutorial – Tomsk: Publishing House of Tomsk Polytechnic University, 2013. - p118.

[3] Favorskaya A.V. Development of numerical methods for modeling the propagation of elastic waves in inhomogeneous media. Abstract, Moscow – 2015.

[4] Sabitova D.S., Zhuzbayev S.S., Juzbayeva B.G. Development of an information analysis system for analyzing wave processes in a homogeneous medium // International Journal of Mechanical Engineering and Technology. – 2018. – Vol. 9(12). – P. 499-508.

[5] Zhuzbayev S., Sabitova D., Sarsenov B. Computer mathematical modeling of wave processes // 4th International conference on computer and technology applications (ICCTA). – Istanbul, 2018. – P. 1-5.

[6] Zhuzbayev S.S., Adilova A.K. Introduction to mathematical modeling. International Conference: The Scientific Thought of the Information Age. Poland, 2018.

[7] Zhuzbayev S.S., Sabitova D.S, Adilova A.K. The use of information-analytical systems for the analysis of wave processes. Scientific conference of mathematicians of Kazakhstan "Actual problems of mathematics", Turkestan, 2018, p.159-162.

[8] Barashkov V.N., Smolina I.Yu., Puteeva L.E., Pestsov D.N. Theory of elasticity: Abstract/ Tomsk: Publishing House Tom. state architect build un, 2012, p.184.

[9] Zhuzbayev S.S., Bayteliev T.B. The method of bi-characteristics in spatial problems of the linear theory of heredity.// Abstracts of the All-Union Symposium on Rheology of Soils. Volgograd, 1985, p. 37-38.

[10] Zhuzbayev S.S. Study of wave processes in heterogeneous structures using computational and descriptive techniques. Abstracts of the II Republican Conference on Computational Mathematics and Research Automation, Almaty, 1988, v4, p42.

[11] Zhuzbayev S.S, Karimbaev T.D. Dynamic deformation of a quarter plane with an elastic insert under lateral impulse loading. // Manuscript №2722, Bibl. Indication of VINITI, scientific works, M., 1989, №11 (2117), p.175.

[12] Zhuzbayev S.S., Bayteliev T.B., Muratalin N.K. Analysis of wave processes in an elastic and elastic-porous medium with an elastic insert. \\Theses of reports to the All-Union scientific and practical conferences Loess subsidence soils as the basis of buildings and structures. Book 3, Barnaul, 1990, p120.

[13] Zhuzbayev S.S., Bayteliev T.B., Yugay O.K. Investigation of the influence of pile driving depths on the stress-strain state of the foundation. // Abstracts of the All-Union Coordination Meeting - Seminar "Mechanized non-waste technology for the construction of pile foundations. Vladivostok, 1991, 2 section, Interaction of pile structures with base soil and stresses arising in piles when driven into the ground. №49, p12.

[14] Zhuzbayev S.S, Karimbaev T.D. Complex stress state at the base of a pile under cyclic loading. // Abstracts of the scientific and technical conference “Strength of materials and structural elements at sound and ultrasonic loading frequencies”, Kiev, 1992, p18.

[15] Zhuzbayev S.S. On pulling out elastic inclusions from an elastic semibounded matrix. // Abstracts of the scientific and technical conference of the MCTU named after Yasavi, Turkestan, 1994, p20.

[16] Tarabrin G.T. The use of the bicharacteristics method for solving non-stationary problems of the dynamics of anisotropic massifs. //M., Structural Mechanics and Structural Analysis, 1981, No. 4, p. 38 - 43.

ISSN: 1992-8645 www.jatit.org E-ISSN: 1817-3195

[17] Tarabrin G.T. Difference schemes of wave problems of the theory of elasticity: monograph /G.T.Tarabrin; Volgograd State Technical University. - Volgograd: RPK "Polytechnic", 2000. - 148 p.

[18] Tarabrin G.T. Methods of mathematical physics. Publishing House Association of Construction Universities, 2009.

[19] Zhuzbayev S, Akhmetova Z, Tleukenov S, Bayenova G. Application of the Splitting Method for the Numerical Solution of Non-Stationary Problems of Elastic Medium Dynamics. The 4th Abu Dhabi University Annual International Conference Mathematical Science and its Applications. December 23–26, 2015.

[20] Akhmetova Z, Boranbayev S, Zhuzbayev S, Sarsenov B. Development of the System with Component for the Numerical Calculation and Visualization of Non-Stationary Waves Propagation in Solids. IOS Book Series: Frontiers in Artificial Intelligence and Applications (FAIA), 2016, Volume293, pp. 353-359, ISSN 0922-6389

[21] Akhmetova Z, Zhuzbaev S, Boranbayev S. The method and software for the solution Of dynamic waves propagation problem in elastic medium.*ActaPhysicaPolonica A*, Polish Academy of Sciences, 130, 2016, pp. 352–354.

[22] Akhmetova Z, Boranbayev S, Zhuzbaev S. The visual representation of numerical solution for a non-stationary deformation in a solid body. Advances in Intelligent Systems and Computing, Switzerland: Springer International Publishing, 448, 2016, pp. 473–482.

[23] Tarabrin, G.T. The Jump Bend, Conversion of convexity thru click: monograph. Saarbrucken (Germany): LAP Lambert Academic Publishing, 2014.

[24] Kukudzhanov, V. N. Numerical Continuum Mechanics. In: De Gruyter Studies in Mathematical Physics, xviii, 2012.